# Supplementary Material for:
# Climatological, Virological, and Sociological Drivers of Current and Projected Dengue Fever Outbreak Dynamics in Sri Lanka

Caroline E. Wagner,[1,2] Milad Hooshyar,[2,3] Rachel E. Baker,[1,2]
Wenchang Yang,[2,4] Nimalan Arinaminpathy,[5] Gabriel Vecchi,[2,4] C. Jessica E. Metcalf,[1]
Amilcare Porporato,[2,4] Bryan T. Grenfell[1,6*]

[1]Department of Ecology and Evolutionary Biology, Princeton University, Princeton NJ 08544, USA
[2]Princeton Environmental Institute, Princeton University, Princeton NJ 08544, USA
[3]Department of Civil and Environmental Engineering, Princeton University, Princeton NJ 08544, USA
[4]Department of Geosciences, Princeton University, Princeton NJ 08544, USA
[5]Department of Infectious Disease Epidemiology, Imperial College School of Medicine, London, UK
[6]Fogarty International Center, National Institutes of Health, Bethesda MD 20892, USA

*To whom correspondence should be addressed; E-mail: grenfell@princeton.edu.

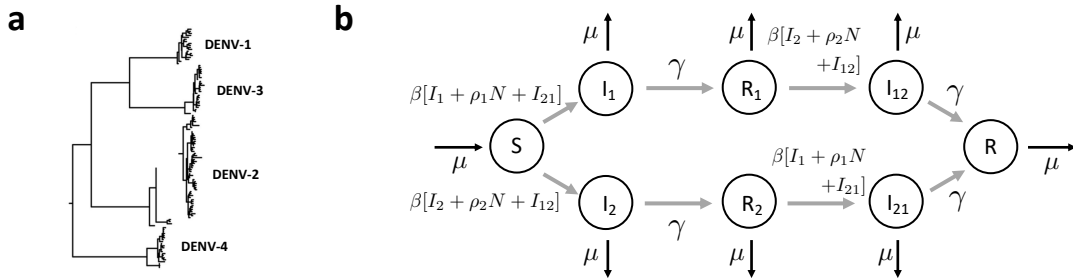## S1  Schematic of the two-strain SIR model



**Figure S1:** (a) Phylogeny of dengue virus from [1]. (b) Schematic of the simplified two-strain SIR model used to characterize serotype invasion based on that developed in [2].

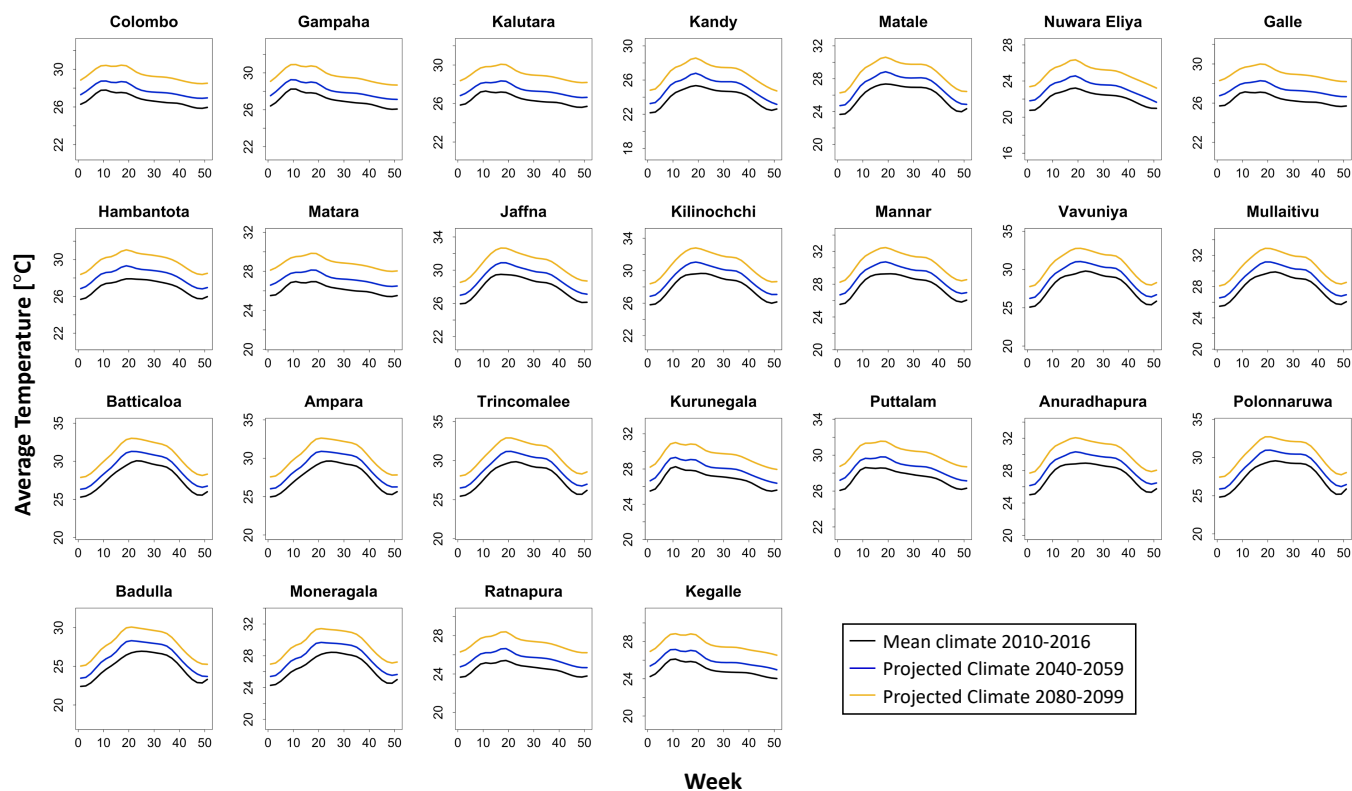# S2    District-level climate data and projections



**Figure S2:**  Annual variation and seasonality of average temperature for all 25 districts of Sri Lanka. Present-day values obtained from the mean climate of the years 2010-2016 are shown as the black curve, and projected values for the time periods 2040-2059 and 2080-2099 are shown as the blue and yellow curves, respectively.

**Figure S3:** Annual variation and seasonality of precipitation for all 25 districts of Sri Lanka. Present-day values obtained from the mean climate of the years 2010-2016 are shown as the black curve, and projected values for the time periods 2040-2059 and 2080-2099 are shown as the blue and yellow curves, respectively.
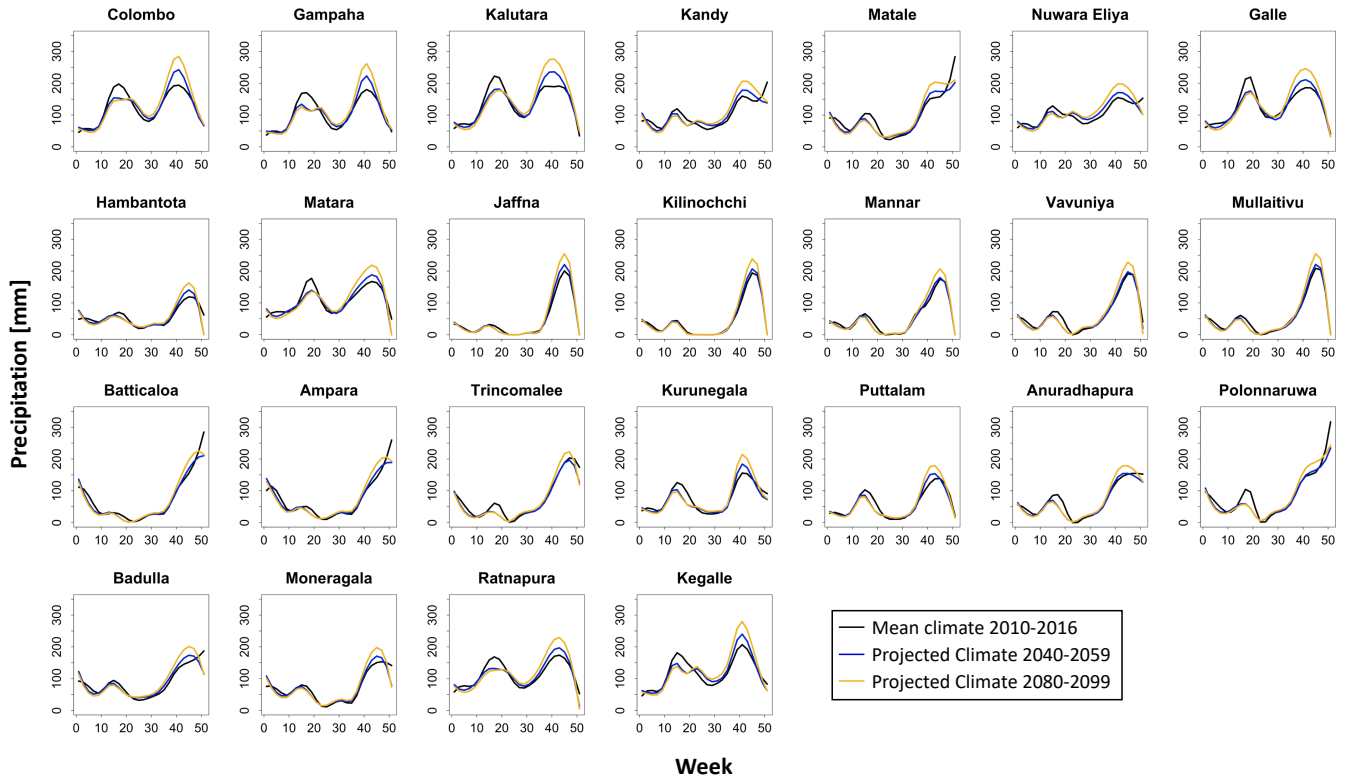
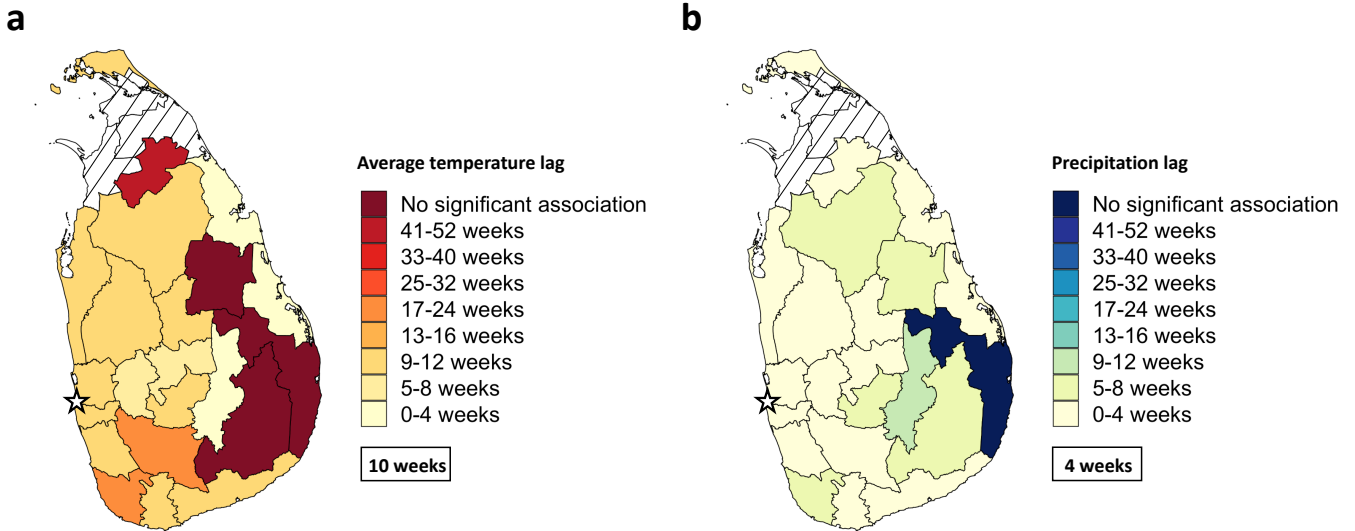# S3   District-specific lag times for climate variables



**Figure S4:** District-specific lag time maximizing the cross-correlation function between empirical transmission rate and (a) average temperature or (b) precipitation. The 3 districts (Kilinochchi, Mannar, and Mullaitivu) excluded from the panel regression model and the determination of the national climatological lag values (see the Materials and Methods section of the main text) are indicated by the dashed lines. The approximate location of the national capital city of Colombo is indicated by the star in each figure.

## S4  Functional forms of the climate variables for the panel regression model
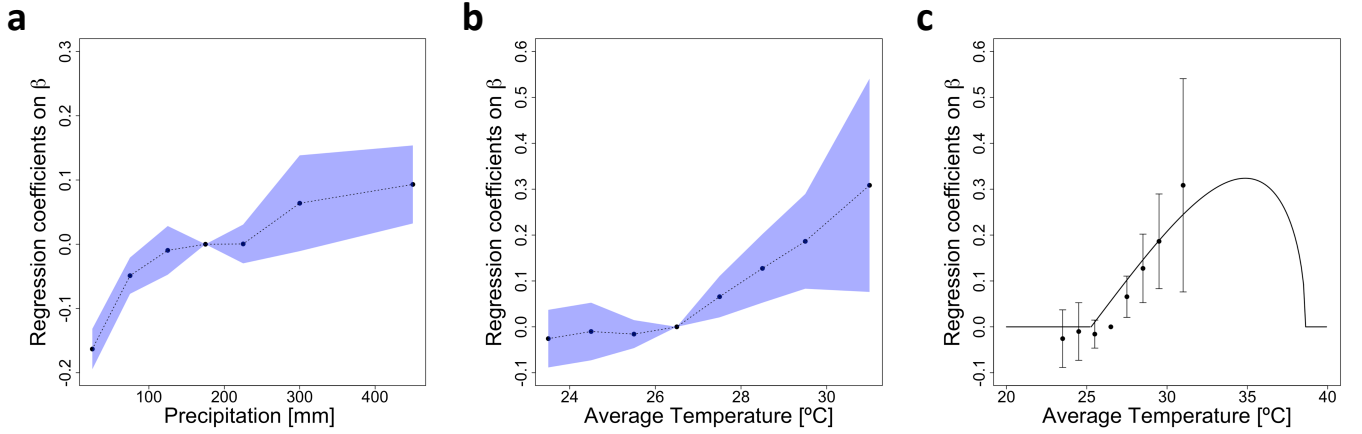


**Figure S5:** Determination of the functional forms for the climate variables in the panel regression model. In (a) and (b), the results from the regression model in Equation (4) of the Materials and Methods section of the main text for the effect of precipitation and temperature, respectively, on log transmission using a flexible binned model are shown. In each case, a linear relationship was assumed in Equation (4) for the non-binned climate variable. The 95% confidence intervals are shown by the blue ribbon. In (c), the results from (b) are fit to the Brière curve in Equation (5) of the Materials and Methods section of the main text with $T_{\max} = 38.63°C$ imposed as the maximum temperature. It is assumed that beyond the fitted maximum and minimum temperatures there is no effect of average temperature of log transmission.

## S5  Results of the panel regression models

|  | Dependent variable: | |
| --- | --- | --- |
|  | $\log(\beta + 1)$ | |
|  | (1) | (2) |
| $f_{\text{Brière}}(\text{Tavg}_{\text{lag}})$ | 1.626e+00*** | |
|  | (3.052e-01) | |
| $\text{Tavg}_{\text{lag}}$ | | 5.910e-02*** |
|  | | (1.137e-02) |
| $\text{Precip}_{\text{lag}}$ | 8.138e-04*** | 8.337e-04*** |
|  | (7.469e-05) | (7.463e-05) |
| Observations | 3,982 | 3,982 |
| $R^2$ | 0.937 | 0.937 |
| Adjusted $R^2$ | 0.930 | 0.930 |
| *Note:* | *p<0.1; **p<0.05; ***p<0.01 | |

**Table S1:** Regression of climate variables on log transmission according to Equation (4) of the Materials and Methods section of the main text for both candidate regression models: (1) a linear response in precipitation and a Brière functional form for average temperature, and (2) linear responses in both average temperature and precipitation.

# S6 Predictions of future transmission rates using a linear climatological model

In Figure S6 we plot the predicted mean empirical $\beta$ values accounting for future climate conditions using the regression model with *linear* average temperature as a comparison for those plotted in Figure 6a of the main text using the regression model with a Brière functional form for Tavg. Note that location-by-month and location-by-year dummies for the three districts that were excluded from the panel regression model (see the Materials and Methods section of the main text) were obtained by re-running the panel regression model with all districts included. The coefficients on the climate variables used for the transmission rate projections for these three districts, however, were set to those obtained by the regression model when these three districts were excluded.
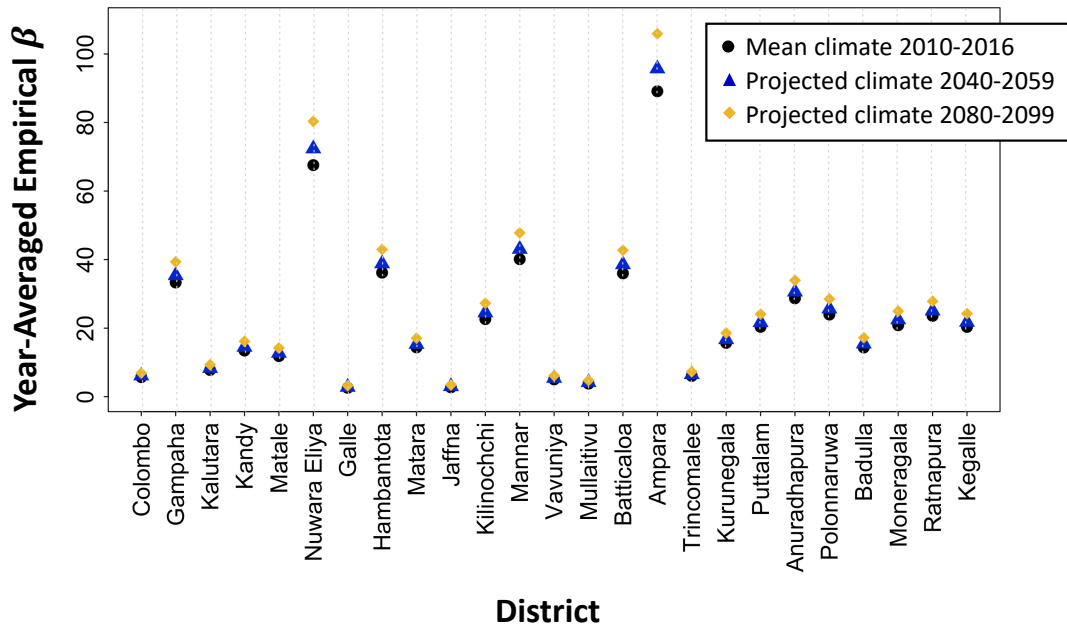


**Figure S6:** Mean annual empirical dengue transmission rates by district obtained from the panel regression model of Equation (4) of the main text assuming a linear dependence of log transmission on both average temperature and precipitation. The present-day values obtained using the mean climate data from 2010 to 2016 are shown as the black circles. Future mean transmission rates obtained from projections of average temperature and precipitation are shown for the time periods 2040-2059 (blue triangles) and 2080-2099 (yellow diamonds).

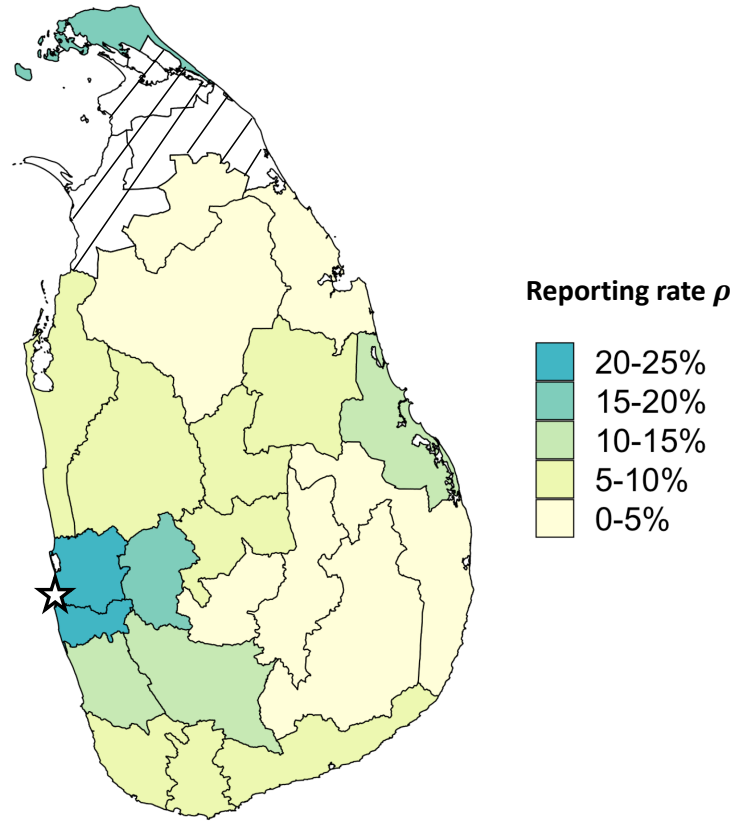# S7  TSIR estimates of district-specific reporting rates



**Figure S7:** Estimated constant-time reporting rate $\rho$ by district obtained from the TSIR model fits to the case data from 2010-2016 using a linear regression model for susceptible reconstruction. The 3 districts (Kilinochchi, Mannar, and Mullaitivu) excluded from the panel regression model and the determination of the national climatological lag values (see the Materials and Methods section of the main text) are indicated by the dashed lines. The approximate location of the national capital city of Colombo is indicated by the star.

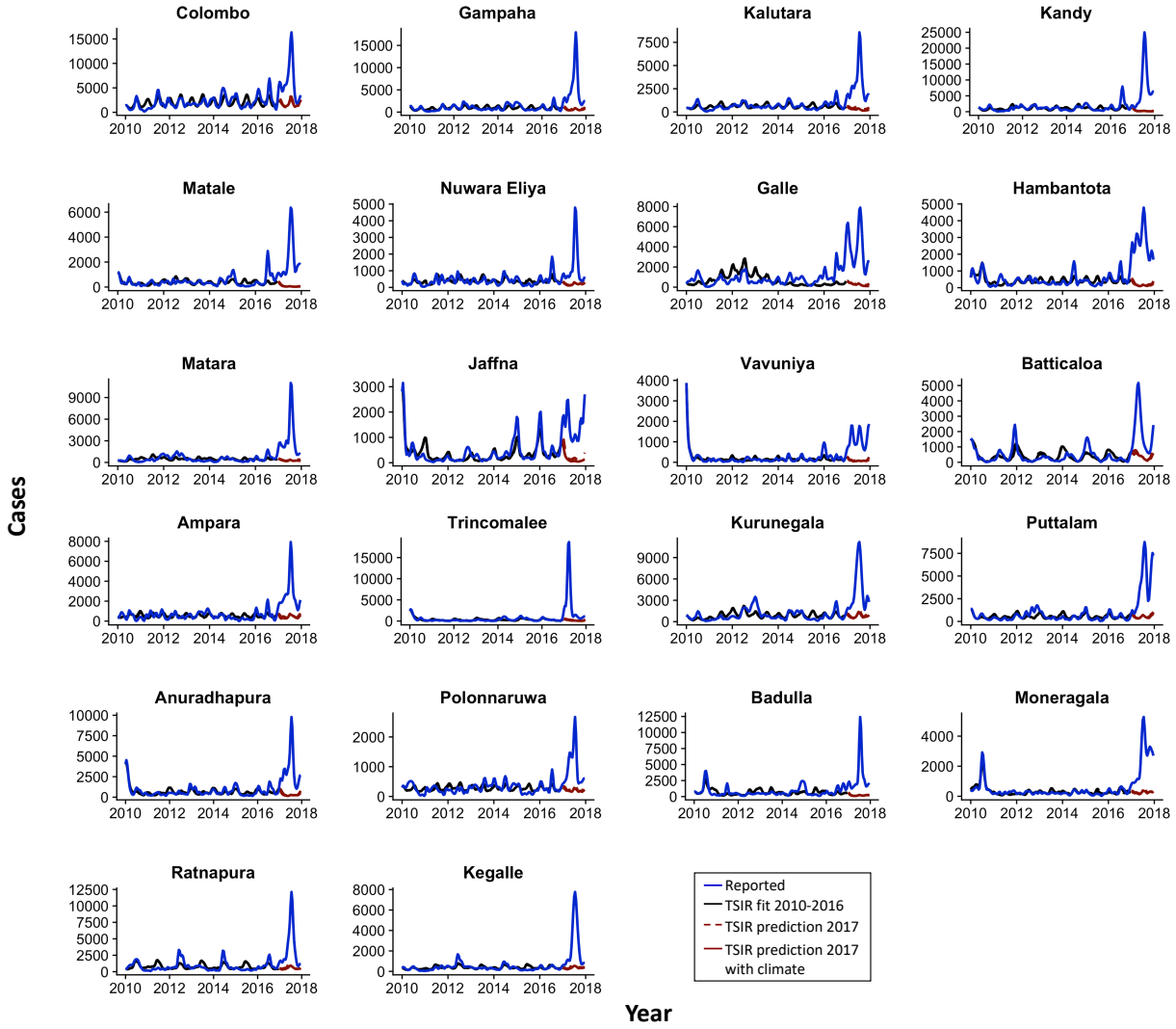# S8 TSIR predictions for 2017 case numbers with climatology by district



**Figure S8:** Dengue cases from 2010 to 2017 adjusted by the reporting rate $\rho$ obtained from the TSIR model fit to the case data from 2010 to 2016 (solid blue line), TSIR model fit from 2010 to 2016 (solid black line), and TSIR predictions for 2017 (dashed red line) for all districts. The solid red line corresponds to the TSIR predictions for 2017 explicitly accounting for the climate of 2017 by deriving the transmission rate from the panel regression model.

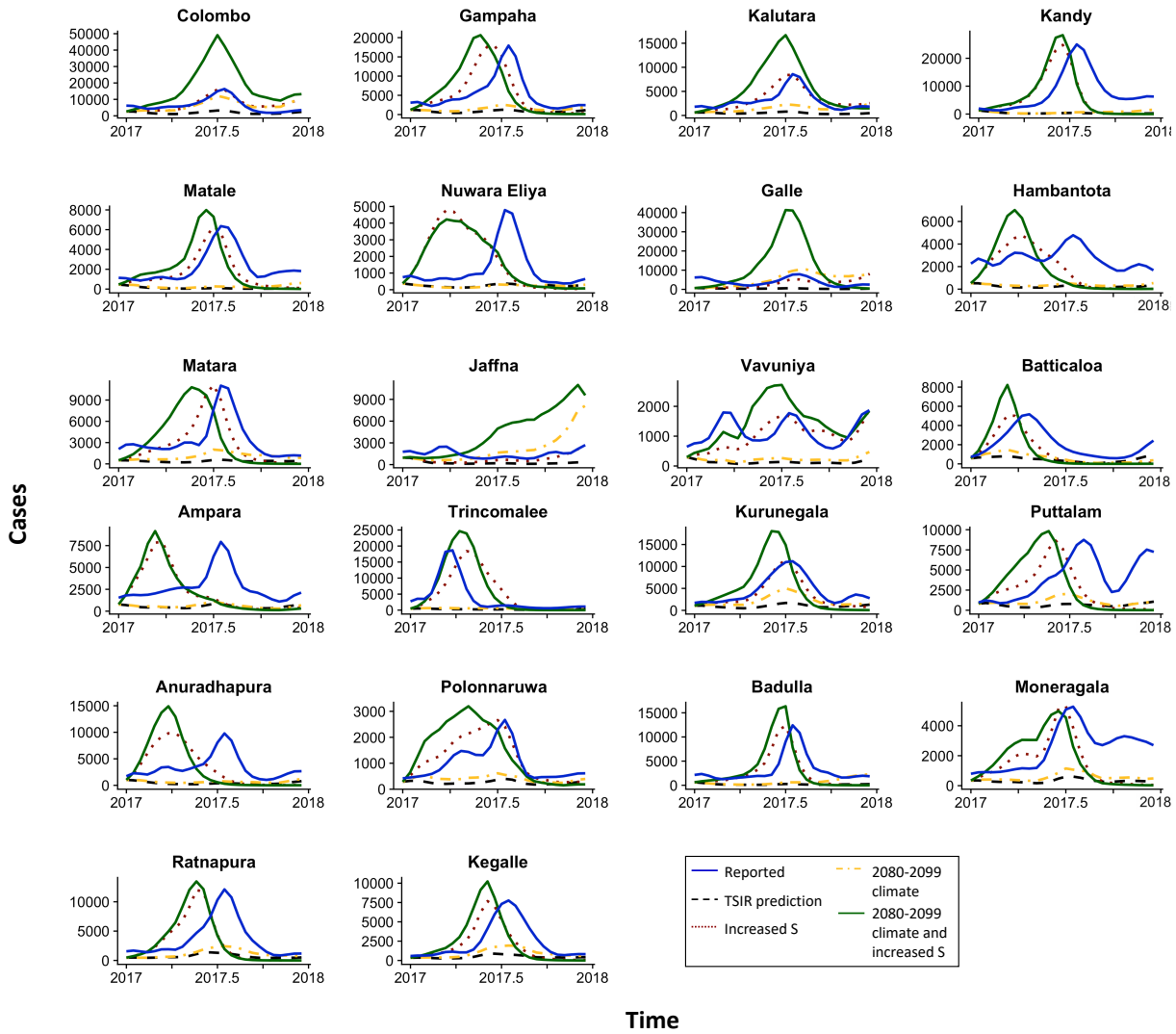# S9　Projections for future transmission dynamics by district



**Figure S9:** Dengue cases for 2017 adjusted by the reporting rate $\rho$ obtained from the TSIR model fit to the case data from 2010 to 2016 (solid blue line) and TSIR predictions for the number of infected individuals for 2017 following training on 2010-2016 data only (dashed black line) for all districts. The TSIR predictions for 2017 under the conditions of increased initial number of susceptible individuals, utilization of the transmission rate derived from the 2080-2099 climate projection data, and both climate and serotype adjustments are shown as the dotted red, dashed-dotted yellow, and solid green lines, respectively.

# References

[1] B. T. Grenfell, O. G. Pybus, J. R. Gog, J. L. N. Wood, J. M. Daly, J. A. Mumford, and E. C. Holmes. Unifying the epidemiological and evolutionary dynamics of pathogens. *Science*, 303(5656):327–332, 2004.

[2] M. Aguiar, S. Ballesteros, B. W. Kooi, and N. Stollenwerk. The role of seasonality and import in a minimalistic multi-strain dengue model capturing differences between primary and secondary infections: Complex dynamics and its implications for data analysis. *Journal of Theoretical Biology*, 289(1):181–196, 2011.